Contents lists available at ScienceDirect

# The International Journal of Biochemistry & Cell Biology

# Caspase-independent apoptosis, in human MCF-7c3 breast cancer cells, following photodynamic therapy, with a novel water-soluble phthalocyanine

Natalia B. Rumie Vittar[a], Josefina Awruch[b], Kashif Azizuddin[c], Viviana Rivarola[a,*]

[a] Departamento Biología Molecular, Facultad de Ciencias Exactas, Universidad Nacional de Río Cuarto, Ruta 8 Km 601, Río Cuarto, Argentina
[b] Departamento de Química Orgánica, Facultad de Farmacia y Bioquímica, Universidad de Buenos Aires, Junín 956, 1113 Buenos Aires, Argentina
[c] Department of Radiation Oncology, Case Western Reserve University School of Medicine and the Case Comprehensive Cancer Center, 10900 Euclid Avenue, Cleveland, OH 44106-4942, USA

## ABSTRACT

A new water-soluble phthalocyanine derivative, *2,3,9,10,16,17,23,24-octakis(3-aminopropyloxy) phthalo-cyaninato zinc II* (*PoII*) was studied as a photosensitizer for photodynamic therapy (PDT) in MCF-7c3 cells. We report here that PoII and red light induces apoptosis. However, the precise mechanism appears to differ from that induced by PDT with other known phthalocyanines. The present study provides evidence that in the case of PoII, caspases do not participate in the apoptotic response. PoII-PDT-treated cells exhibited chromatin condensation and phosphatidylserine (PS) externalization. In the absence of light activation, PoII had no detectable cytotoxic effect. An early event upon PoII-PDT was photodamage to lysosomes, suggesting that they are the primary sites of action. Moreover, the treatment induces Bid activation, mitochondrial swelling and translocation of apoptosis-inducing factor (AIF) to the nucleus. An atypical proteolysis of poly(ADP-ribose) polymerase (PARP) indicative of calpain-like activation was observed. These data support the notion that an alternative mechanism of caspase-independent apoptosis was found in PoII-photosensitized cells.

© 2010 Elsevier Ltd. All rights reserved.

## 1. Introduction

A novel cancer treatment that is receiving increased attention worldwide is photodynamic therapy (PDT). PDT is a binary therapy that involves the combination of visible light and a photosensitizer. Each component is harmless by itself, but in combination with molecular oxygen, together they can lead to the generation of singlet oxygen ($^1O_2$) as well as other reactive oxygen species (ROS), oxidative cell damage and cell death. At the molecular level, direct tumor cell destruction by PDT is caused by irreversible photodamage to vital subcellular targets, which include the plasma membrane and membranes of the mitochondria, lysosomes, Golgi apparatus and endoplasmic reticulum (ER). It is generally accepted that the intracellular localization of the sensitizer coincides with the primary site of photodamage, because the photogenerated $^1O_2$ has a very short half-life and very limited diffusion in biological systems (Buytaert et al., 2007; Oleinick et al., 2001).

The lethal mechanisms initiated by the photosensitization process appear to encompass the three major morphologies of programmed cell death, i.e., apoptotic, necrotic and autophagic cell death (Buytaert et al., 2006a,b; Kessel et al., 2006). The most widely studied of these mechanisms is apoptosis, which has been observed in many tumor cell lines after PDT with a variety of porphyrin, phthalocyanine, and other photosensitizers (Ichinose et al., 2006; Kriska et al., 2005; Usuda et al., 2003).

Apoptosis is an ATP-requiring process morphologically characterized by chromatin condensation, cleavage of chromosomal DNA into internucleosomal fragments, cell shrinkage, membrane blebbing, formation of apoptotic bodies without plasma membrane breakdown, exposure of phosphatidylserine (PS) in the outer leaflet of the plasma membrane, and phagocytosis by neighboring cells. At the biochemical level, apoptosis most commonly entails the activation of caspases. It is generally accepted that once activated, the effector caspases are responsible for most of the stereotypic morphological and biochemical changes observed during apoptosis by cleaving a restricted subset of vital substrates (Luthi and Martin, 2007).

However, emerging evidence from an increasing number of experimental systems demonstrates a mechanism in which apoptosis can occur independently of caspase activation. Cell death in these systems often occurs with only partial condensation of chromatin and without internucleosomal DNA fragmentation, but it

maintains many other features of apoptosis (Almeida et al., 2004; Broker et al., 2005).

Known mitochondrial inducers of caspase-independent cell death are the flavoprotein apoptosis-inducing factor (AIF) and the endonuclease Endo G. These inter-mitochondrial membrane space (IMS) pro-apoptotic proteins are released into the cytosol following the permeabilization of mitochondrial membranes and are thought to translocate to the nucleus where they are involved in DNA fragmentation and chromatin condensation in a caspase-independent fashion (van Loo et al., 2002). Recent studies have implicated the mitochondrial release of AIF as a key mediator of caspase-independent apoptosis following PDT (Furre et al., 2005, 2006).

The mechanism by which these proteins are released from mitochondria is under the tight control of the Bcl-2 family of pro- and anti-apoptotic proteins that elicit opposing effects on mitochondria (Borner, 2003).

Caspase-8 was the first protease shown to be responsible for Bid processing (Li et al., 1998). However, now it is clear that cleavage of Bid can be achieved by several other proteases in a caspase-independent manner, including the serine protease Granzyme B (Alimonti et al., 2001), lysosomal proteases (Stoka et al., 2001), and calpain (Mandik et al., 2002). Once processed, tBid translocates to mitochondria and induces mitochondrial membrane permeabilization and the release of apoptotic factors. Evidence from many studies supports the concept that cell death can proceed in a caspase-independent manner while maintaining the key characteristics of apoptosis (Broker et al., 2005; Lemarié et al., 2004).

The substrates for some caspases are known and include the DNA repair enzyme poly(ADP-ribose) polymerase (PARP). Caspases-3 and -7 cleave the 113-kDa PARP at a specific aspartic acid to generate two fragments of 90 and 23 kDa. However, when two human breast cancer cell lines were exposed to beta-lapachone, an atypical PARP fragmentation produced a 60-kDa fragment instead of the typical 89 kDa and this alteration was thought to involve the activation of a calpain-like protease (Pink et al., 2000).

The aim of the present study was to evaluate the efficacy of PoII photosensitization to induce an apoptotic response in human breast cancer cells and to analyze the cellular mechanisms involved in this process. Using a variety of criteria, we demonstrate that a novel photosensitizer, the water-soluble phthalocyanine PoII, induces a caspase-independent apoptosis in the human breast cancer cell line MCF-7.

## 2. Materials and methods

### 2.1. Cell culture and photodynamic treatment

The human breast cancer MCF-7 (WS8) cell line transfected with the pBabepuro retroviral vector encoding human procaspase-3 cDNA (here referred to as MCF-7c3 cells) was provided by Dr. C.J. Froelich (Northwestern University, Evanston, IL). The cells were cultured in RPMI 1640 medium containing 10% fetal bovine serum (FBS) and $2 \mu g/mL$ puromycin. The cultures were maintained at $37 \,^{\circ}C$ in a humidified atmosphere of 5% $CO_2$–95% air. The phthalocyanine photosensitizer PoII [2,3,9,10,16,17,23,24-octakis(3-aminopropyloxy)phthalocyaninato zinc] was synthesized as previously described (Strassert et al., 2005), and used as a 0.1 mM stock solution in distilled water. Cells were incubated with $1 \mu M$ PoII in medium containing 4% FBS for 18 h. Prior to photoirradiation of cells, the dye-containing medium was replaced with fresh medium. The light source was a light-emitting diode array (EFOS, Mississauga, Ontario, Canada) delivering light with the following parameters: $\lambda_{max} \sim 670$–675 nm; $1 \,mW/cm^2$; up to $1 \,J/cm^2$.

Irradiation was carried out at room temperature, followed by incubation of the cultures in the dark at $37 \,^{\circ}C$ for various periods of time.

### 2.2. Determination of cellular PoII content

Cellular sensitizer content was determined in the cell extracts using a fluorometric assay. Briefly, $5 \times 10^5$ cells were seeded out in $10$-$cm^2$ Petri dishes, and incubated with $1 \mu M$ PoII for 18 h. At the end of incubation, cell monolayers were washed with PBS ($3 \times$) and then 3 mL of 1% SDS was added. Fluorescence of the cell extracts was measured at PoII excitation and emission peak (580 and 683 nm, respectively), in a Perkin-Elmer LS fluorometer. Appropriate controls were used to subtract fluorescence not originating from the extracted sensitizer.

### 2.3. Determination of cell survival

Cells were seeded into $25$-$cm^2$ flasks and allowed to grow until the cell density reached $(1–2) \times 10^6$ cells per flask. Some of the cultures were exposed to PDT. The cells were collected from the monolayer with trypsin, and aliquots were plated in triplicate into 6 cm Petri dishes in amounts sufficient to yield 50–100 colonies per dish. After incubation for 13–14 days, the cells were stained with 0.1% crystal violet in 20% ethanol, and colonies containing at least 50 cells were counted.

### 2.4. Nuclear staining for detection of apoptotic cells

To assess the changes in nuclear morphology typical of apoptosis, MCF-7c3 cells were cultured in 35 mm culture plates. At different time points following PDT, cells grown on coverslips were fixed in PBS containing 3.7% formaldehyde. After rinsing twice with PBS, cells were stained with $1$–$5 \mu g/mL$ Hoechst 33342 (Molecular Probes) for 15 min at room temperature. Cells were then washed $2 \times$ with PBS and subsequently immersed in a mounting medium containing anti-fade reagent (Molecular Probes) and visualized under a Leitz Laborlux fluorescence microscope. Apoptotic cells were determined by the characteristic chromatin condensation, margination and fragmentation.

### 2.5. DNA content and phosphatidylserine exposure in PDT-treated cells

At different time points following PDT, cells were collected from the monolayer with trypsin, and fixed with 1% formaldehyde (in PBS) for 15 min on ice. Cells were then washed $2 \times$ with PBS, treated with 0.2% Triton X-100 for 5 min on ice, centrifuged, and resuspended in staining buffer ($25 \mu g/mL$ propidium iodide (PI), and $100 \mu g/mL$ RNase) for 30 min. Cells were kept on ice until DNA content analysis, which was carried out in the Flow Cytometry Facility of the Case Comprehensive Cancer Center (He et al., 1996). To detect phosphatidylserine (PS) externalization, MCF-7c3 cells were harvested by trypsinization and washed $2 \times$ with PBS. Washed cells were resuspended in $200 \mu L$ binding buffer (100 mM HEPES, pH 7.4, 140 mM NaCl, 2.5 mM $CaCl_2$). Annexin V-Pe ($3 \mu g/mL$, Medical and Biological Laboratories CO, LTD) and 7AAD (7-amino-actinomycin D, $3 \mu g/mL$, Molecular Probes) were added according to the manufacturer's instructions. After incubation for 15 min, $400 \mu L$ binding buffer were added, and samples were analyzed using an EPICS ESP flow cytometer (Coulter Corp.) with excitation by a 488-nm argon ion laser. 7AAD was added to samples to distinguish necrotic and late apoptotic events (annexin V−, 7AAD+; annexin V+, 7AAD+) from early apoptotic events (annexin V+, 7AAD−).

## 2.6. Preparation of cell extracts for SDS-PAGE, and immunoblotting analysis

Cells were lysed and sonicated, and cellular protein was denatured, as described (Xue et al., 2001). The protein content of the lysate was measured using BCA protein assay reagent (Pierce), and aliquots containing equivalent amounts of protein were loaded onto 12% polyacrylamide gels, subjected to electrophoresis, transferred to PVDF membranes, and incubated with one of the following antibodies: monoclonal anti-caspase-3 (Transduction Laboratories, Lexington, KY); monoclonal anti-caspase-9 (Transduction Laboratories, Lexington, KY); polyclonal anti-procaspase-3 (Pharmingen); anti-caspase-8 (Pharmingen); anti-Bid (Santa Cruz, Santa Cruz, CA); polyclonal anti-AIF (Santa Cruz Biotechnology, INC); polyclonal anti-calpain (Santa Cruz Biotechnology, INC); monoclonal anti-PARP (Pharmingen); anti-actin (Amersham, Arlington Heights, IL). The immune complexes were detected by enhanced chemiluminescence (ECL) system (Amersham).

## 2.7. Analysis of caspase 8 activity in PDT-treated cells

Cells were tested for caspase-8 activity by a colorimetric assay (BD Clontech). For the assay, $2 \times 10^6$ cells from each sample were lysed and tested for cleavage of IETD-pNA caspase-8 substrate according to the manufacturer's instructions. The released fluorescence was measured in a Perkin-Elmer LS50 fluorometer.

## 2.8. Determination of lysosomal disruption and mitochondrial swelling

Cells were cultured in glass-bottomed 35 mm Petri dishes. To monitor lysosomal disruption after treatment, cells were first incubated with PoII for 18 h and before irradiation loaded with 100 nM LysoTracker Green DND-26 (Molecular Probes) for 45 min at 37 °C. Subsequently, the dye-containing medium was refreshed, and the cultures were photoirradiated. Confocal images were collected using 488 nm excitation light from an argon/krypton laser and a 500–550 nm band-pass filter. Lysosome staining pattern was quantified by software (ImageJ, www.nih.org).

To assess mitochondrial swelling, cells grown on cover slips were incubated with 1 μM PoII for 18 h at 37 °C. Prior to photoirradiation, MitoTracker Green FM (100 nM, Molecular Probes) was added. Following 3× PBS washes, fluorescence images were acquired with a Zeiss Axiophot microscope (Carl Zeiss, Germany). Images were captured using an AxioCam HRc (Carl Zeiss, Germany) camera and subsequently processed using AxioVision Rel. 4.3 software.

## 2.9. Immunofluorescent staining of AIF

For detecting AIF, cells grown on cover slips were formaldehyde-fixed after PDT treatments, 0.2% Triton X-100 permeabilized and incubated with blocking solution containing 2% bovine serum albumin (BSA) in PBS. Cells were incubated overnight at 4 °C with primary antibody (1:100; rabbit polyclonal AIF (Santa Cruz Biotechnology, INC)) diluted in 0.1% Triton X-100 in PBS (PBS-T) and then with secondary antibody, FITC-conjugated anti-rabbit IgG. The cover slips were mounted on slides and examined with a Zeiss fluorescence microscope.

## 2.10. Pulsed-field gel electrophoresis (PFGE)

Total cellular DNA was isolated from treated cultures and analyzed for its size distribution as described previously (He et al., 1996).

# 3. Results and discussion

## 3.1. PoII enters the cells and photosensitizes them

The localization of the photosensitizer is of special importance, since it determines the primary site of damage. While singlet oxygen has a very short lifetime in cells, its intracellular targets are located close to the sites where the sensitizer is located. Therefore, cellular structures having sensitizer will be preferentially damaged upon illumination. Hence, it is not surprising that the type of response triggered by activation of the photosensitizer depends on its intracellular localization (Juarranz et al., 2004; Rumie Vittar et al., 2008). Uptake of PoII by MCF-7c3 cells was measured by comparing the fluorescence of PoII in solution and in cell extracts. As shown in Fig. 1A, the presence of PoII in the cell extracts was observed by the typical phthalocyanine emission with a maximum at 683 nm (Strassert et al., 2005), indicating that the sensitizer was taken up by the cells.

To establish the photocytotoxicity of PoII-PDT on MCF-7c3 cells, we conducted a clonogenic assay, which measures the ability of each cell in the culture to maintain all the functions needed to divide and form a colony. Cell survival was not affected by light or PoII, but when cells were exposed to the combination of 1 μM PoII incubation followed by irradiation with light doses ranging from 0.5 to 20 J/cm², decrease of cell survival from 92% to 30% was observed (Fig. 1B).

## 3.2. Condensed chromatin, sub-G1 DNA content and PS externalization after PoII-PDT

Next, the effect of PoII-sensitized PDT on the occurrence of apoptosis was examined. Because the rate of apoptosis increased with both PDT dose and post-treatment time, cells were collected early and late after treatment. At 24 h after PDT, irradiation with a light dose of 10 J/cm² produced few cells with the nuclear changes indicative of apoptosis, but when the fluence was increased to 20 J/cm², more cells with condensed chromatin and DNA fragmentation were found, reaching a maximum of about 60%. Representative images are shown in Fig. 2A, and the calculated percentages of nuclei with condensed chromatin in Fig. 2B. The yield of apoptotic cells increased from 24 to 72 h when cells were exposed to light doses lower than 20 J/cm², indicating that the rate of the apoptotic process was PDT dose-dependent.

The induction of apoptosis was confirmed and quantified by flow cytometry (Fig. 2C). Frequency distribution histograms of DNA content of PoII-PDT-treated cells show an increase in the population of cells with less than the G1 content of DNA, corresponding to apoptotic cells and a reduction of the G1 and G2 peaks within 24 h after irradiation at 10 J/cm². These results suggest that this dose of PoII-PDT activated the apoptotic response, although apoptotic nuclear morphology was not observed until 72 h after light exposure (Fig. 2B).

The redistribution of plasma membrane PS is an early marker of apoptosis (Di Stefano et al., 2001). Since Annexin V-Pe can also detect necrotic cells as a result of the loss of membrane integrity, apoptotic cells were differentiated from necrotic cells by an increase in 7AAD positivity, which selectively labels necrotic but not apoptotic cells. To monitor the time course of PS exposure, Annexin V-Pe binding and 7AAD uptake were measured by flow cytometry. The increase of PS translocation occurred by 24 h post-irradiation with 10 and 20 J/cm², and this increase was more pronounced at 48 h after exposure (Fig. 2D). Concomitantly, there was an increase in positivity for 7AAD, suggesting that some cells had lost membrane integrity and were in late apoptosis or necrosis. Taken together, the data of Fig. 2 indicate that photodamaged cells are in apoptosis but that the three indicators such as chro-
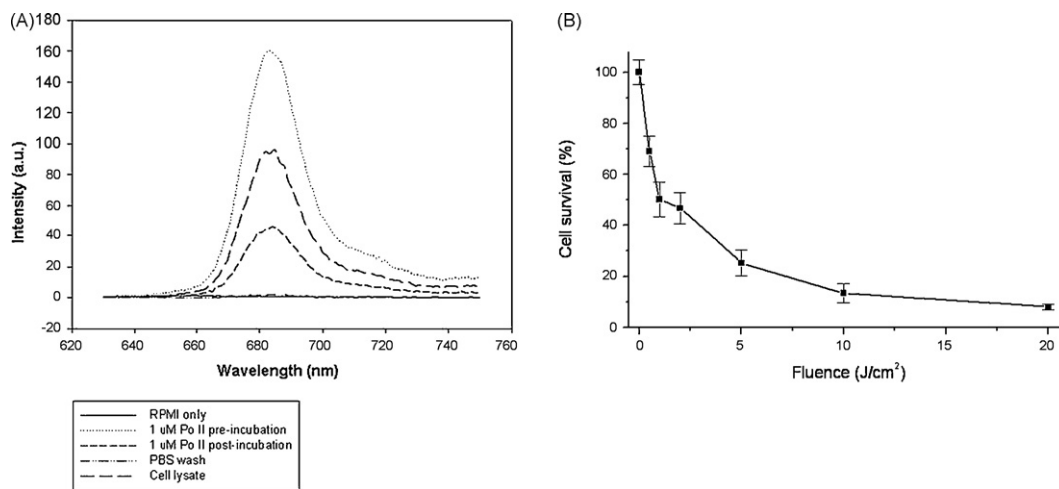
**Fig. 1.** PoII emission spectrum and loss of clonogenicity of MCF-7c3 cells following PDT. (A) Emission spectra of RPMI cell culture medium, medium with the addition of 1 μM PoII (preincubations); and medium after 18 h incubation with MCF-7c3 cells (post-incubation). PBS washes (to remove unbound PoII); and lysed cells ($\lambda_{exc}$ = 610 nm). (B) Exponentially growing cultures were incubated with 1 μM PoII for 18 h and then irradiated with various red light doses. Immediately after irradiation, cells were collected by trypsinization, and the appropriate numbers were plated into 100 mm dishes. Colonies were stained and counted 10–12 days after plating. Controls consisted of cells exposed to light only, PoII only or no treatment. Cell survival was not affected by light or Po II alone; therefore, all control values were averaged, and the experimental values were normalized to the mean plating efficiency, which varied between 86 and 82% in these experiments. Data represent the mean ± SD of duplicate plates from three independent experiments.

matin condensation, externalization of plasma membrane PS, and the appearance of cells or cell fragments containing less than the G1 content of DNA are visualized at 24, 48 and 72 h after PDT treatment, respectively.

### 3.3. Caspases-8, -9, and -3 do not participate in the apoptotic response to PoII-PDT

Apoptosis can be triggered by two major pathways, intrinsic and extrinsic. The most commonly observed pathways of apoptosis after PDT involve the activation of a cascade of caspases, most prominently caspases-8, -9, and -3, that cleave a series of proteins leading to the endpoints shown in Fig. 2. Therefore, we next asked whether these caspases participate in apoptosis following PoII-PDT. In the intrinsic pathway, cytochrome c released from mitochondria into the cytosol complexes with apoptosis-activation factor 1, procaspase-9, and dATP to form the "apoptosome", which initiates the cleavage and activation of procaspases-9 and -3 (Xue et al., 2001). As monitored by Western blots, we did not observe any processing of procaspase-9 to the active enzyme in MCF-7c3 cells in response to PoII-PDT (Fig. 3A).

The activation of caspase-3 requires its proteolytic processing from the 32-kDa pro-enzyme to the 17-kDa active enzyme. Cell lysates from MCF-7c3 cultures undergoing apoptosis did not show active 17 kDa caspase-3 (Fig. 3A). However, in cell treated with 1 μM STS or Pc4-PDT inducers, the 17-kDa fragment of active caspase-3 was clearly detected. Indeed, in cells Jurkat treated with STS were employed as an additional control to locate the position of the cleavage fragment (Fig. 3A). The lysates were also tested for the enzymatic activity of caspase-3; no activity above that of the controls was detected consistent with the Western blot analysis (data not shown). Furthermore, there was no evidence of loss of procaspase-3 in response to PoII-PDT (Fig. 3B). Induction of apoptosis can be triggered by cell-surface death receptors that lead to caspase-8 activation through the extrinsic pathway. As shown in Fig. 3C, no procaspase-8 cleavage was observed, as indicated by bands at the position of the inactive fragment. Moreover, Fig. 3D shows that at all time points investigated, PoII-PDT was not able to induce caspase-8 enzymatic activity.

### 3.4. Lysosomal damage, Bid cleavage and mitochondrial swelling after PoII-PDT

Another important factor in PDT is the intracellular distribution of the drug, and this may be responsible for differences in the photosensitizing efficiency and mechanism with different phthalocyanines. In order to evaluate the PoII photoinjury on key organelles we have focused our attention on lysosomes and mitochondria of the photosensitized cells. A key factor in determining the type of cell death is the magnitude of lysosomal permeabilization and the amount of proteolytic enzymes released into the cytosol. Whereas partial, selective permeabilization triggers apoptotic-like programmed cell death, massive breakdown of lysosomes results in unregulated necrosis (Broker et al., 2005). So as summarized in Fig. 4A, typical lysosome labeling pattern (marked by punctuate green fluorescent dye) was observed in control cells. However, 15 min after PDT the green punctate staining was strongly decreased and replaced by diffuse green fluorescence showing that in most cells the lysosome-specific pattern was completely abolished. More substantial alterations were detected after a PDT dose of 20 J/cm², concomitant with nuclear condensation that revealed cells undergoing apoptosis. Evidence of photodynamic action on this organelle was less extensive with a dose of 10 J/cm², and this correlated well with the small fraction of apoptotic cells found within the first hours after PDT. Analysis of the green particles (pixels) in the fluorescent pictures is a quantitative representation of the decrease of lysosome-specific pattern (Fig. 4A, lower panel).

It is known that the chlorine photosensitizer ATX-s10 localizes into lysosomes, and the apoptotic response to photoinjury can be prevented by pharmacological inhibition of lysosomal proteases (Ichinose et al., 2006). Also, we have reported that S1, a zinc phthalocyanine derivate, was partially localized in lysosomes, and this compartment represented its primary photodamage site leading to apoptosis in PDT-treated MCF-7c3 cells (Rumie Vittar et al., 2008). The release of proteases from photodamaged lysosomes can catalize the proteolytic activation of Bid (Reiners et al., 2002), and this cleavage can be also achieved by other proteases (Mandik et al., 2002). Another apoptotic signaling pathway is initiated by cell-membrane death receptors and mediated by caspase-8, that once activated can cleave the Bcl-2 homolog Bid, which acts on mitochondria to release pro-apoptotic proteins (Grinberg et al., 2002).
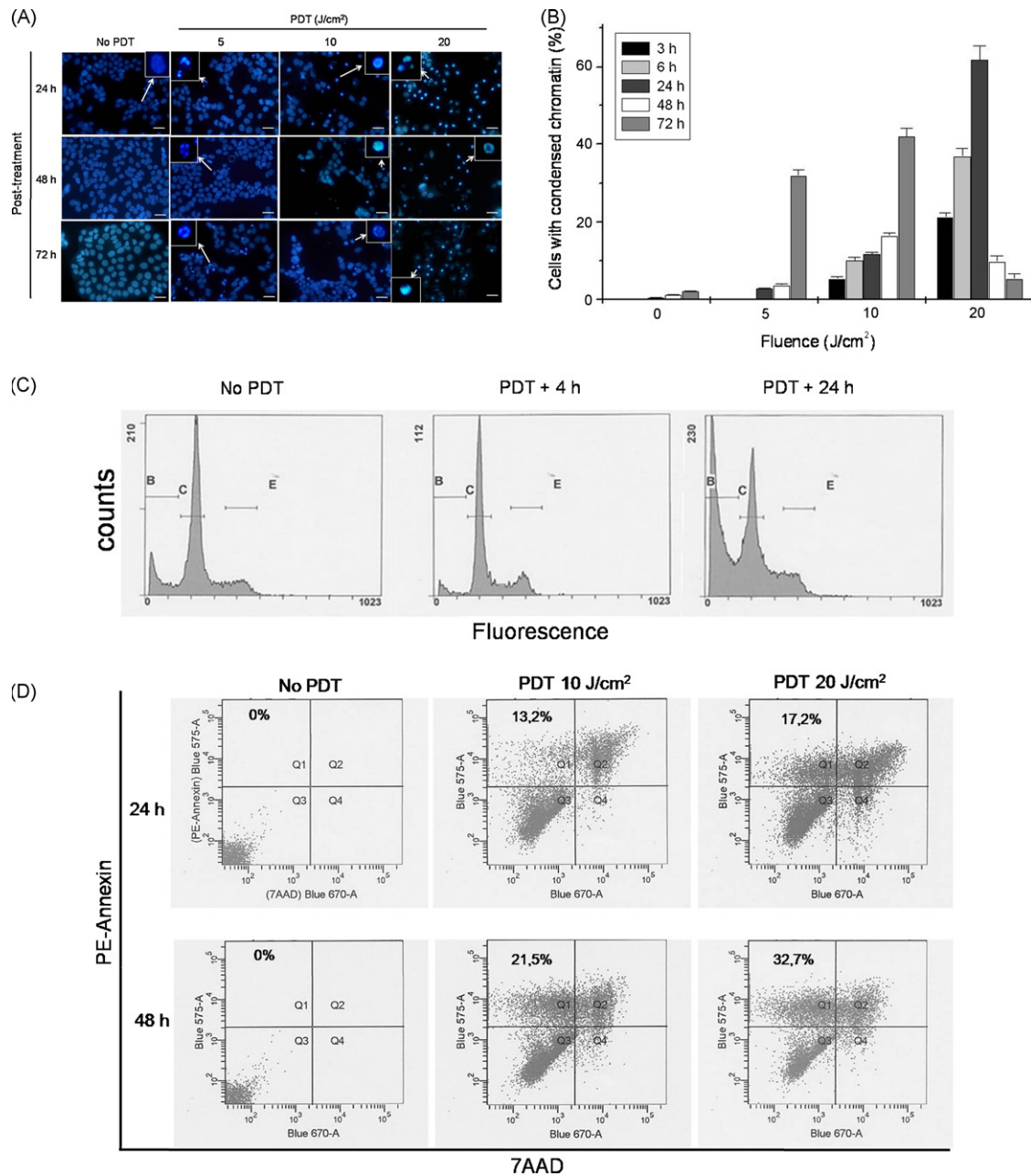
**Fig. 2.** The progression of apoptosis in MCF-7c3 cells after PDT. (A and B) Cells growing on cover slips were treated with PDT or not; at various times thereafter, the cells were fixed, stained with Hoechst 33342, and visualized by fluorescence microscopy. (A) Representative micrographs from PDT-treated and untreated cells. Arrows indicate enlarged nuclei. (B) Percentages of cells containing nuclei with apoptotic features were calculated for a range of fluences and times after PDT. Data represent the mean ± SD of at least 200 cells from each cover slip from three experiments. (C and D) Flow cytometric determination of apoptotic cells as those with less than the G1 content of DNA or those with PS externalized. (C) Frequency distribution histograms of DNA content from PI-stained MCF-7c3 cells after PDT. The cells were treated with 1 μM PoII for 18 h and exposed to 10 J/cm² of red light. Samples were removed for assay at indicated time after irradiation: (B) subdiploid population, (C) diploid population and (D) bivariate flow cytometry dot plots of Annexin V-stained vs. 7AAD-stained MCF-7c3 cells. Cells were incubated with 1 μM PoII and exposed to light dose 10 or 20 J/cm² and then analyzed 24 and 48 h post-PDT. The lower left quadrant (PE-Ann−/7AAD−) represents viable cells, while the upper left (PE-Ann+/7AAD) and right (PE-Ann+/7AAD+) quadrants show apoptotic and necrotic cells or late apoptotic cells, respectively. PS: phosphatidyserine.

We analyzed the time course of Bid activation by WB (Fig. 4B). In parallel experiments we observed mitochondrial changes following PoII-PDT assessed by fluorescent microscopy (Fig. 4C). Levels of the cleavage product of Bid were detectable as loss of the full-length form at 3 h after treatment. At the latest time point (9 h) maximum cleavage was observed as a residual faint band of under-graded Bid (Fig. 4B). To visualize the mitochondria structure during PDT treatment, cells were incubated with MitoTracker® Green FM, a green fluorescent probe, which is taken up by the polarized mitochondria and is suitable to monitor mitochondrial volume changes under conditions that produce mitochondrial depolarization (Ferreira et al., 2004). As shown in Fig. 4C, control cells presented tubular elements distributed over the whole cytoplasm. Analysis of irradiated cells 3 h after PDT, demonstrated alterations of tubular elements which began round and increased in diameter. These alterations increased up to 24 h, and this stage cells had fully swollen mitochondria and had entered the execution phase of apoptosis.

An examination of the typical mitochondrial-labeling pattern indicates that photodynamic treatment using PoII induced
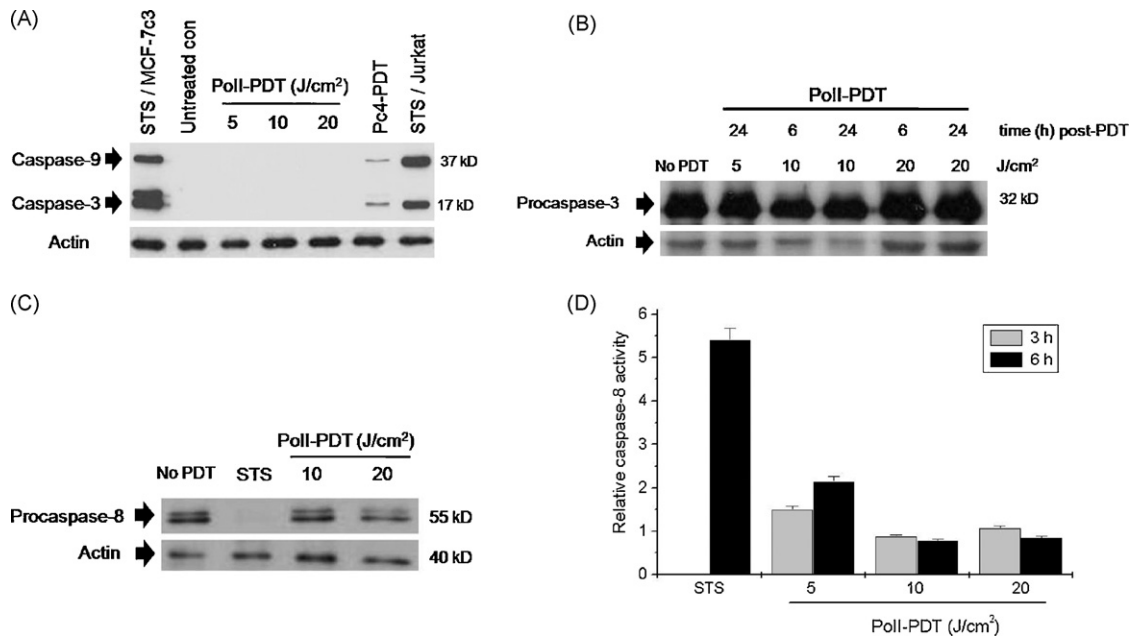
**Fig. 3.** Effect of PoII-PDT on caspase activation. MCF-7c3 cells were incubated 18 h with 1 μM PoII and then exposed to different light doses (5, 10, and 20 J/cm²). Whole cell lysates were prepared at 24 h after irradiation. (A) Immunoblot detection of caspase-3 and -9. As positive controls, STS (Staurosporine) treated MCF-7c3 and Jurkat cells, and Pc4-PDT-treated MCF-7c3 cells were used. Equal amount of protein (50 μg/lane) from each treatment were separated by SDS-PAGE and subsequently transferred to PVDF membranes. (B) Immunoblot of procaspase-3. (C) Immunoblot analysis of procaspase-8. Whole cell lysates were prepared 6 h after PoII-PDT or STS addition and analyzed for the level of procaspase-8. (D) Enzymatic activity of caspase-8 as measured by the cleavage of a fluorogenic substrate by cell lysates prepared 3 or 6 h after PoII-PDT or 6 h after addition of STS. Data were normalized to lysates of untreated cells.
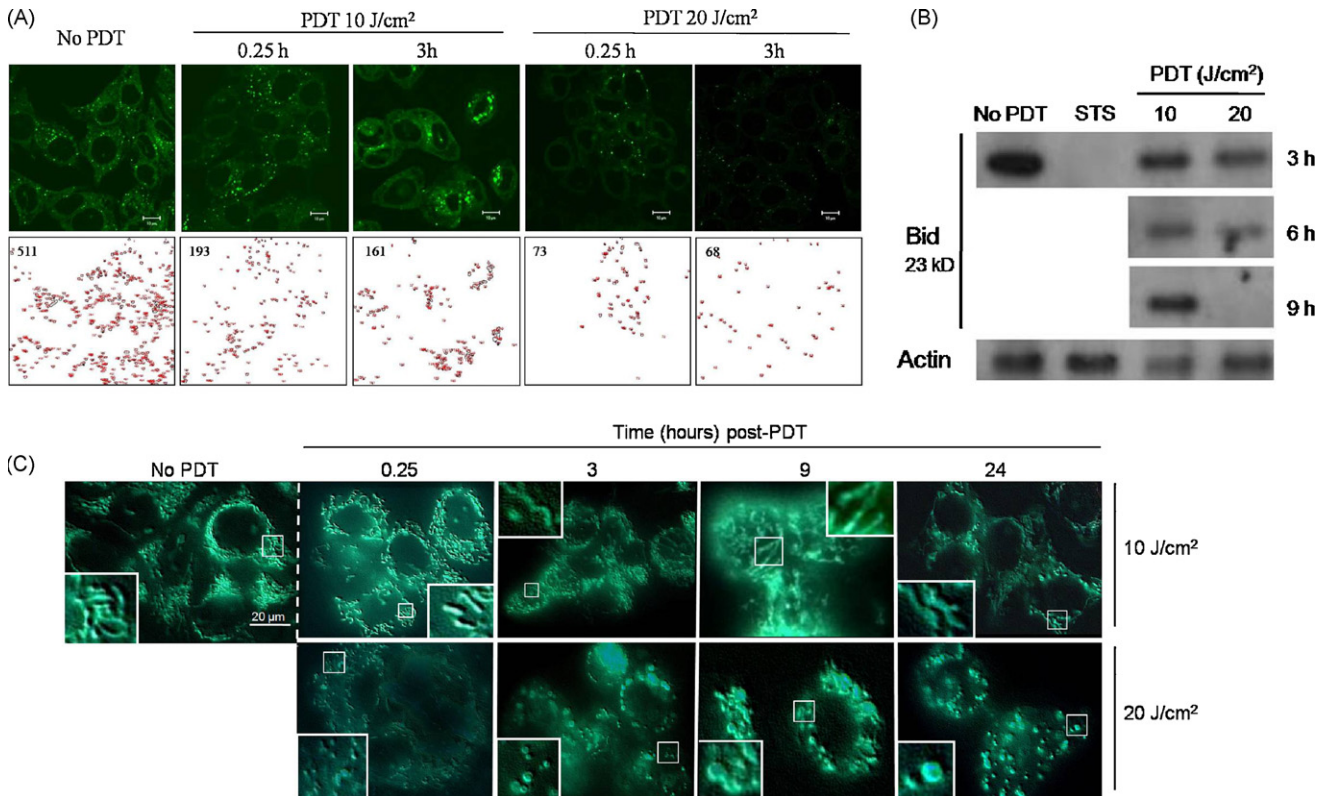


**Fig. 4.** PoII-PDT leads to lysosomal damage, Bid activation and mitochondrial swelling. (A) Analysis of lysosomal integrity after PDT. MCF-7c3 cells were treated with 1 μM PoII at 37 °C for 18 h, refed and irradiated (10–20 J/cm²). At the indicated times after irradiation, cells were stained with Lyso-Tracker Green DND-26 (500 nM) probes to visualize lysosomes. Non-treated cultures (No PDT) were processed similarly. Scale bar, 10 μm. (Lower panel) Green pixels of the representative picture (A) were analyzed by the software ImageJ. The values of green decreased in both time- and dose-dependent manner. Representative fluorescent images from one of three independent experiments are presented. (B) Effect of PoII-PDT on the expression of pro-apoptotic protein Bid. Whole extract from PDT-treated MCF-7c3 cells were prepared and analyzed at 3, 6, and 9 h after light treatment (10 or 20 J/cm²) by Western blot with anti-Bid antibody. STS-treated MCF-7c3 cells were used as positive controls. (C) Mitochondrial changes after PoII-PDT. Cells were loaded with 50 nM MitoTracker Green FM at 37 °C for 20 min and then exposed to PoII-PDT. Square in the micrograph indicates magnifications. Note greater diameter of the mitochondria after treatment compared with no PDT. Representative fluorescent images from one of three independent experiments are presented. (For interpretation of the references to color in this figure legend, the reader is referred to the web version of the article.)
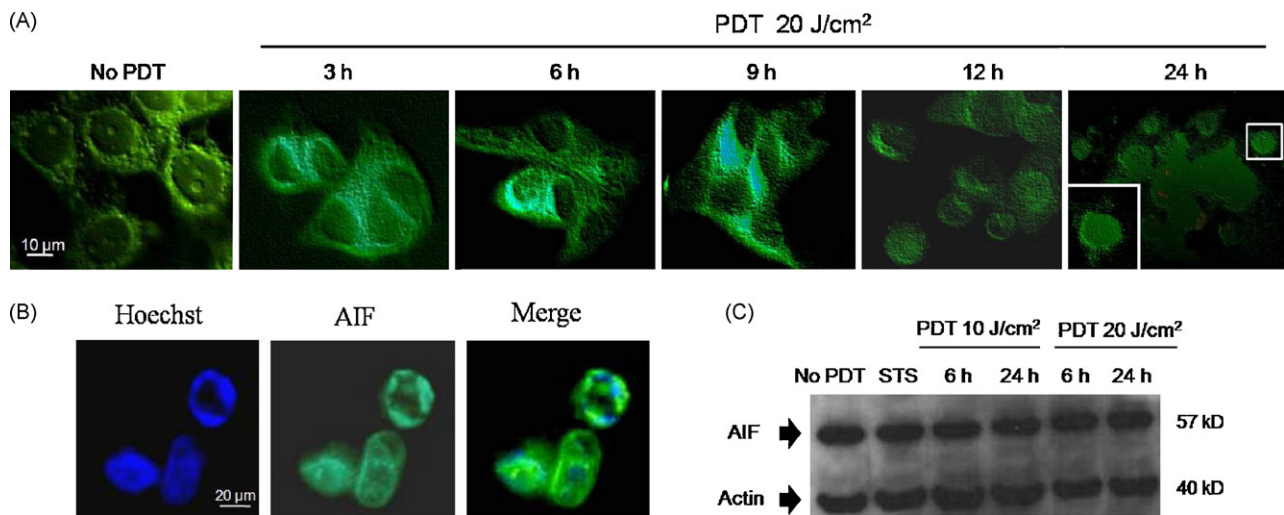
**Fig. 5.** AIF nuclear translocation after PoII-PDT. PDT-induced nuclear translocation of AIF (A and B) was demonstrated by immunofluorescent staining. (A) MCF-7c3 cells were treated with (PDT) or without (No PDT) 1 μM PoII at 37 °C for 18 h. After treatment, cells were subjected to immunofluorescent staining. Note that untreated control cells (without PDT) lack any detectable AIF redistribution to the nucleus. Representative fluorescent images from one of five independent experiments are presented. (B) AIF nuclear staining 24 h after PDT dose (1 μM PoII + 20 J/cm$^2$). Panel: left, nuclear staining by Hoechst; center, FITC-AIF; right, merge. Scale bar, 20 μm. (C) Immunoblot analysis of AIF in MCF-7c3 cells. MCF-7c3 cells were treated with or without PoII-PDT. Whole cell extracts was prepared, separated by 12% SDS-PAGE and probed with antibodies specifically against AIF. Actin was used as internal control for equal cell input. STS: staurosporine.

mitochondrial alterations indicative of membrane depolarization. Similar result was reported by Lam et al. (2001).

These experiments suggest the activation of Bid does play a key role in the regulation of mitochondrial integrity, because it can be detected concomitantly with depolarization. PoII is taken up by MCF-7c3 cells, and based on the confocal images and spots quantification, illumination with visible light caused dye loss from lysosomes, due to lysosomal membrane permeabilization. Because of the absence of caspase-8 mediated cleavage under this experimental condition, it is possible that the release of lysosomal proteases to cytosol precedes tBid formation.

### 3.5. AIF translocation and increased calpain expression in PoII-PDT

During apoptosis, the strict compartmentalization of potentially lethal proteins such as cytochrome c, cathepsins, and AIF is selectively disrupted. Numerous studies using photodynamic treatments show the collapse of mitochondrial membrane potential after therapy resulting in the release of apoptogenic factors (Grebenova et al., 2003; Huang et al., 2005). In recent a years, it has became increasingly evident that in many experimental situations AIF is released from mitochondria and triggered apoptosis in a caspase-independent fashion. Also, it has been demonstrated that AIF causes chromatin condensation and large-scale (∼50 kbp) DNA fragmentation (Arnoult et al., 2003).

Immunofluorescence detection of AIF using a FITC conjugate (green fluorescence) normally yields a punctuate cytoplasmic staining pattern with some preference for the perinuclear area. As response to PoII photosensitization process, AIF staining showed a diffuse pattern in the cytoplasm and some in the nuclear regions (Fig. 5A), and at 24 h after PDT treatment, AIF staining was strongly detected in the nucleus (Fig. 5A and B). It should be noted that the interpretation of AIF immunofluorescence data is complicated because the intensity of AIF staining increases considerably upon translocation to the cytosol, but is clearly observed to be present in the nucleus, whereas the immunoblot analysis does not support the increase in the total amount of the protein (Fig. 5C).

Several studies demonstrated that AIF is anchored to the outer face of the mitochondrial inner membrane, precluding its release following loss of outer membrane integrity. To be released from mitochondria, AIF needs to be cleaved into tAIF by calpain or cathepsins (Polster and Fiskum, 2004; Polster et al., 2005; Yuste et al., 2005). On the other hand, Bid is cleaved by calpain, as well as by caspases, into a truncated form with higher activity (Chen et al., 2001). Therefore, the ability of calpain to release AIF in the presence of Bid could be due to calpain-mediated enhancement of Bid-induced pore size, enabling AIF passage, or to increased access of calpain to the intermembrane space, enabling direct cleavage of AIF by calpain (Polster et al., 2005).

Changes in calpain expression following PDT were investigated by Western blotting. At 3 h after PDT, the level of calpain-specific fragment was similar to that of the control cells. It increased by 9 h and reached the highest level 24 h after PDT photosensitization (Fig. 6A). There is strong evidence suggesting that calpain activity downstream of Bid cleavage is required for AIF release and Bid alone did not promote its discharge from mitochondria. Interestingly, PARP is a direct substrate for calpain and undergoes calpain-dependent cleavage under certain conditions of neuronal apoptosis. To further confirm the functional activity of calpain after PDT, Western blotting was performed to determine the specific product of PARP cleavage (Boland and Campbell, 2003; Planchon et al., 2001). When MCF-7c3 cells were exposed to PoII-PDT, little or no PARP typical-fragment from caspase cleavage was observed at all doses tested, confirming once again, that caspases do not participate in PoII-PDT apoptotic response. However, a 60-kDa fragment was found when PDT was performed with a light dose of 20 J/cm$^2$, coinciding with the observed increased in calpain band and the highest percentage of nuclei with apoptosis-like condensation. As shown in Fig. 6B, our findings correlate well with Planchon et al. (2001) and suggest that the cleavage product of PARP would be generated by calcium-related event via calpain-like protease activation. Our results demonstrated that calpain-like proteases could be mediating signals through mobilization of pro-apoptotic factors in a caspase-independent manner.

In the current set of experiments, an increase in DNA fragmentation was observed at 24 h after PoII photosensitization (Fig. 7). These data strongly imply AIF apoptogenic function.

To sum up, we hypothesize the following mechanism: PoII-PDT causes a sequence of events which include photodamage to lyso-
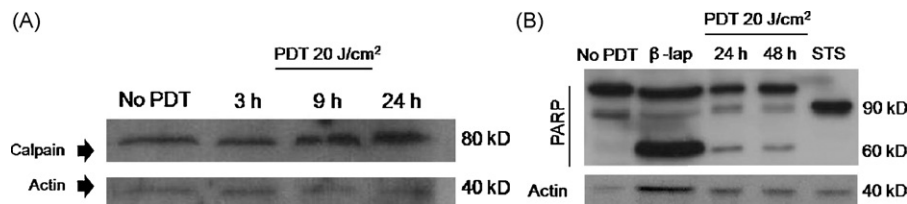
(A)



(B)

**Fig. 6.** Immunoblot analysis of calpain activation in PolI-PDT. (A) The level of calpain expression was increased within the time frame of the experiment. MCF-7c3 cells were treated with 1 μM PolI at 37 °C for 18 h, refed and irradiated (20 J/cm$^2$). Cell lysates were then separated by 12% SDS-PAGE and probed with antibody against calpain. Actin was used as a loading control. (B) PARP cleavage after PolI-PDT. MCF-7c3 cells were collected following treatment (1 μM PolI + 20 J/cm$^2$) and then analyzed by Western blot with anti-PARP antibody. Note 60 kDa band from PDT treatments was similar to that of β-lap (β-lapachone)-treated cells used as positive for calpain activity. Actin was used as a loading control.
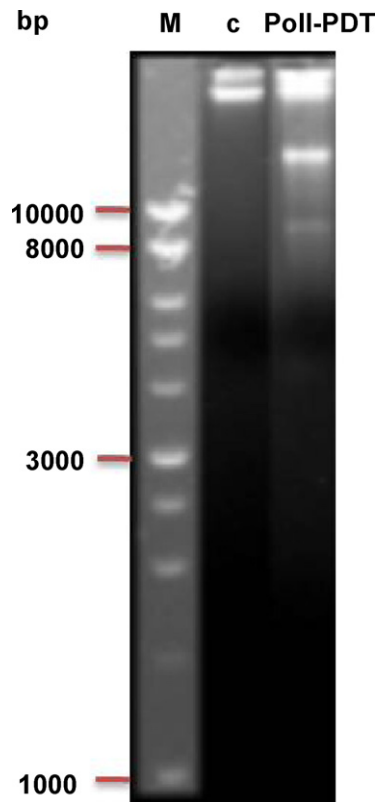


**Fig. 7.** Large-scale DNA fragmentation in response to PolI-PDT. Cells were either untreated (c) or treated with 1 μM PolI overnight and then exposed to 20 J/cm$^2$ (PolI-PDT). After treatment for 24 h, DNA was analyzed by pulsed-field gel electrophoresis. M, size marker.

somes, the release of proteases, cleavage and activation of Bid, the permeabilization of mitochondria and the release of apoptogenic proteins, all in a caspase-independent manner.

## 4. Conclusions

We have characterized the molecular events leading an apoptotic response in human breast cancer cells sensitized by PolI. We argued that this process is modulated in a caspase-independent manner involving lysosomal membrane permeabilization, which in turn promotes cell death by triggering mitochondrial dysfunction and subsequent release of apoptogenic proteins.

The mechanisms connecting mitochondrial membrane permeabilization to the AIF apoptogenic action may include the pro-apoptotic protein Bid and calpain-like protease activity that has been proven following PDT. These data point to an obligatory participation of mitochondria in the transmission of lethal signal initially perceived at the lysosomal level.

Several lines of evidence suggest that although cancer cells may have blocked their normal apoptotic program, cell death can still occur through the release of lysosomal enzymes. It is to note that in our case, PolI-induced PDT efficiently triggered lysosomal cell death pathway, and to our knowledge, this is the first report of a role for calpain in caspase-independent apoptosis in response to stimulus from sensitized lysosomes. Results from the current study not only provide insight into a possible mechanism for PDT-mediated apoptosis, but also raises hopes in the treatment of cancers that are resistant to classic apoptosis inducers. However, whether lysosomal proteases, Bid and calpain pathways are interrelated during PDT-induced AIF release is still unknown and needs to be explored in future studies.

## Acknowledgements

## References

Alimonti JB, Shi L, Baijal PK, Greenberg AH. Granzyme B induces Bid-medited cytochrome c release and miochondrial permeability transition. J Biol Chem 2001;276:6974–82.

Almeida RD, Manadas BJ, Carvalho AP, Duarte CB. Intracellular signaling mechanisms in photodynamic therapy. Biochim Biophys Acta 2004;1704:59–86.

Arnoult D, Gaume B, Karbowski M, Sharpe JC, Cecconi F, Youle RJ. Mitochondrial release of AIF and EndoG requires caspase activation downstream of Bax/Bak-mediated permeabilization. EMBO J 2003;22:4385–99.

Boland B, Campbell V. Beta-amyloid (1–40)-induced apoptosis of cultured cortical neurons involves calpain-mediated cleavage of poly-ADP-ribose polymerase. Neurobiol Aging 2003;24:179–86.

Borner C. The Bcl-2 protein family: sensors and checkpoints for life-or-death decisions. Mol Immunol 2003;39:615–47.

Broker LE, Kruyt FAE, Giaccone G. Cell death independent of caspases: a review. Clin Cancer Res 2005;11:3155–62.

Buytaert E, Callewaert G, Hendrickx N, Scorrano L, Hartmann D, Missiaen L, et al. Role of endoplasmic reticulum depletion and multidomain proapoptotic BAX and BAK proteins in shaping cell death after hypericin-mediated photodynamic therapy. FASEB J 2006a;20:756–8.

Buytaert E, Callewaert G, Vandenheede JR, Agostinis P. Deficiency in apoptotic effectors Bax and Bak reveals an autophagic cell death pathway initiated by photodamage to the endoplasmic reticulum. Autophagy 2006b;2:238–40.

Buytaert E, Dewaele M, Agostinis P. Molecular effectors of multiple cell death pathways initiated by photodynamic therapy. Biochim Biophys Acta 2007;1776:86–107.

Chen M, He H, Zhan S, Krajewski S, Reed JC, Gottlieb RA. Bid is cleaved by calpain to an active fragment *in vitro* and during myocardial ischemia/reperfusion. J Biol Chem 2001;276:30724–8.

Di Stefano A, Ettore A, Sbrana S, Giovanni C, Neri P. Purpurin-18 in combination with light leads to apoptosis or necrosis in HL60 leukemia cells. Photochem Photobiol 2001;73:290–6.

Ferreira SD, Tedesco AC, Sousa G, Zangaro RA, Silva NS, Pacheco MT, et al. Analysis of mitochondria, endoplasmic reticulum and actin filament after PDT with AlPcS4. Lasers Med Sci 2004;18:207–12.

Furre IE, Shahzidi S, Luksiene Z, Møller MTN, Borgen E, Morgan J, et al. Targeting PBR by hexaminolevulinate-mediated photodynamic therapy induces apoptosis through translocation of apoptosis-inducing factor in human leukemia cells. Cancer Res 2005;65:11051–60.

Furre IE, Moller MT, Shahzidi S, Nesland JM, Peng Q. Involvement of both caspase-dependent and-independent pathways in apoptotic induction by hexaminolevulinate-mediated photodynamic therapy in human lymphoma cells. Apoptosis 2006;11:2031–42.

Grebenova D, Kuzelova K, Smetana K, Pluskalova M, Cajthamlova H, Marinov I, et al. Mitochondrial and endoplasmic reticulum stress-induced apoptotic pathway are activated by 5-aminolevulinic acid-based photodynamic therapy in HL60 leukemia cells. J Photochem Photobiol B: Biol 2003;68:71–85.

Grinberg M, Sarig R, Zaltsman Y, Frumkin D, Grammatikakis N, Reuveny E, et al. tBid homoologomerizes in the mitochondrial membrane to induce apoptosis. J Biol Chem 2002;277:12237–45.

He J, Agarwal ML, Larkin HE, Friedman LR, Xue LY, Olelnick NL. The induction of partial resistance to photodynamic therapy by the protooncogene BCL-2. Photochem Photobiol 1996;64:845–52.

Huang HF, Chen YZ, Wu Y. ZnPcS2P2-based photodynamic therapy induces mitochondria-dependent apoptosis in K562 cells. Acta Biochem Biophys Sin 2005;37:488–94.

Ichinose S, Usuda J, Hirata T, Inoue T, Ohtani K, Maehara S, et al. Lysosomal cathepsin initiates apoptosis, which is regulated by photodamage to Bcl-2 at mitochondria in photodynamic therapy using a novel photosensitizer ATX-s10 (Na). Int J Oncol 2006;29:349–55.

Juarranz A, Villanueva A, Soltermann AT, Durantini EN, Espada J, Stockert JC, et al. Photodynamic Therapy: Selective uptake of photosensitizing drugs into tumor cells. Curr Topics Pharmacol 2004;8:185–217.

Kessel D, Vicente MG, Reiners Jr JJ. Initiation of apoptosis and autophagy by photodynamic therapy. Lasers Surg Med 2006;38:482–8.

Kriska T, Korytowski W, Girotti AW. Role of mitochondrial cardiolipin peroxidation in apoptotic photokilling of 5-aminolevulinate treated tumor cells. Arch Biochem Biophys 2005;433:435–46.

Lam M, Oleinick NL, Nieminen AL. Photodynamic therapy-induced apoptosis in epidermoid carcinoma cells. Reactive oxygen species and mitochondrial inner membrane permeabilization. J Biol Chem 2001;276:47379–86.

Lemarié A, Lagadic-Gossman D, Morzadec C, Allain N, Fardel O, Vernhet L. Cadmium induces caspase-independent apoptosis in liver HEP3B cells: role for calcium in signaling oxidative stress-related impairment of mitochondria and relocation of endonuclease G and apoptosis-inducing factor. Free Radic Biol Med 2004;36:1517–31.

Li H, Zhu H, Xu CJ, Yuan J. Cleavage of Bid by caspase 8 mediates the mitochondrial damage in the Fas pathway of apoptosis. Cell 1998;94:491–501.

Luthi AU, Martin SJ. The CASBAH: a searchable database of caspase substrates. Cell Death Differ 2007;14:641–50.

Mandik A, Vikorson K, Strangberg L, Heiden T, Hanson J, Linder S, et al. Calpain-mediated Bid cleavage and calpain-independent Bak modulation: two separate pathways in cisplatin-induced apoptosis. Mol Cell Biol 2002;22:3003–13.

Oleinick NL, Morris RL, Belichenko I. The role of apoptosis in response to photodynamic therapy: what, where, why, and how. Photochem Photobiol 2001;1:1–21.

Pink JJ, Wuerzberger-Davis S, Tagliarino C, Planchon SM, Yang X, Froelich CJ, et al. Activation of a cysteine protease in MCF-7 and T47D breast cancer cells during beta-lapachone-mediated apoptosis. Exp Cell Res 2000;255:144–55.

Planchon S, Pink J, Tagliarino C, Bornmann WG, Varnes ME, Boothman DA. b-Lapachone-induced apoptosis in human prostate cancer cells: involvement of NQO1/xip3. Exp Cell Res 2001;267:95–106.

Polster BM, Fiskum G. Release mechanisms for apoptotic proteins from neural cell mitochondria. J Neurochem 2004;90:1281–9.

Polster BM, Basanez G, Etxebarria A, Hardwick JM, Nicholls DG. Calpain I induces cleavage and release of apoptosis-inducing factor from isolated mitochondria. J Biol Chem 2005;280:6447–54.

Reiners Jr JJ, Caruso JA, Mathieu P, Chelladurai B, Yin X-M, Kessel D. Release of cytochrome c and activation of pro-capase-9 following lysosomal photodamage involves bid cleavage. Cell Death Differ 2002;9:934–44.

Rumie Vittar NB, Prucca CG, Strassert C, Awruch J, Rivarola VA. Cellular inactivation and antitumor efficacy of a new zinc phthalocyanine with potential use in photodynamic therapy. Int J Biochem Cell Biol 2008;40:2192–205.

Stoka V, Turk B, Shendel SL, Kim TH, Cirman T, Snipas SJ, et al. Lysosomal protease pathways to apoptosis. Cleavage of bid, not procaspases, is the most likely route. J Biol Chem 2001;276:3149–57.

Strassert CA, Rodriguez ME, Dicelio LE, Awruch J. A synthetic approach towards novel octasubstituted zinc(II) phthalocyanines with different solubility and photophysical properties. J Porphyrins Phthalocyanines 2005;9:361–7.

Usuda J, Azizuddin K, Chiu SM, Oleinick NL. Association between the photodynamic loss of Bcl-2 and the sensitivity to apoptosis caused by phthalocyanine photodynamic therapy. Photochem Photobiol 2003;78:1–8.

van Loo G, Saelens X, van Gurp M, MacFarlane M, Martin SJ, Vandenabeele P. The role of mitochondrial factors in apoptosis: a Russian roulette with more than one bullet. Cell Death Differ 2002;9:1031–42.

Xue LY, Chiu SM, Oleinick NL. Photodynamic therapy-induced death of MCF-7 human breast cancer cells: a role for caspase-3 in the late steps of apoptosis but not for the critical lethal event. Exp Cell Res 2001;263:145–55.

Yuste VJ, Moubarak RS, Delettre C, Bras M, Sancho P, Robert N, et al. Cysteine protease inhibition prevents mitochondrial apoptosis-inducing factor (AIF) release. Cell Death Differ 2005;12:1445–8.